Standardising Bioassays for Spatial Emanators against Mosquito Vectors

Walter Fabricio Silva Martins[1], Timothy Hill[1], Rosemary Susan Lees[1]

[1]Department of Vector Biology, Liverpool School of Tropical Medicine - LSTM, Liverpool, UK.

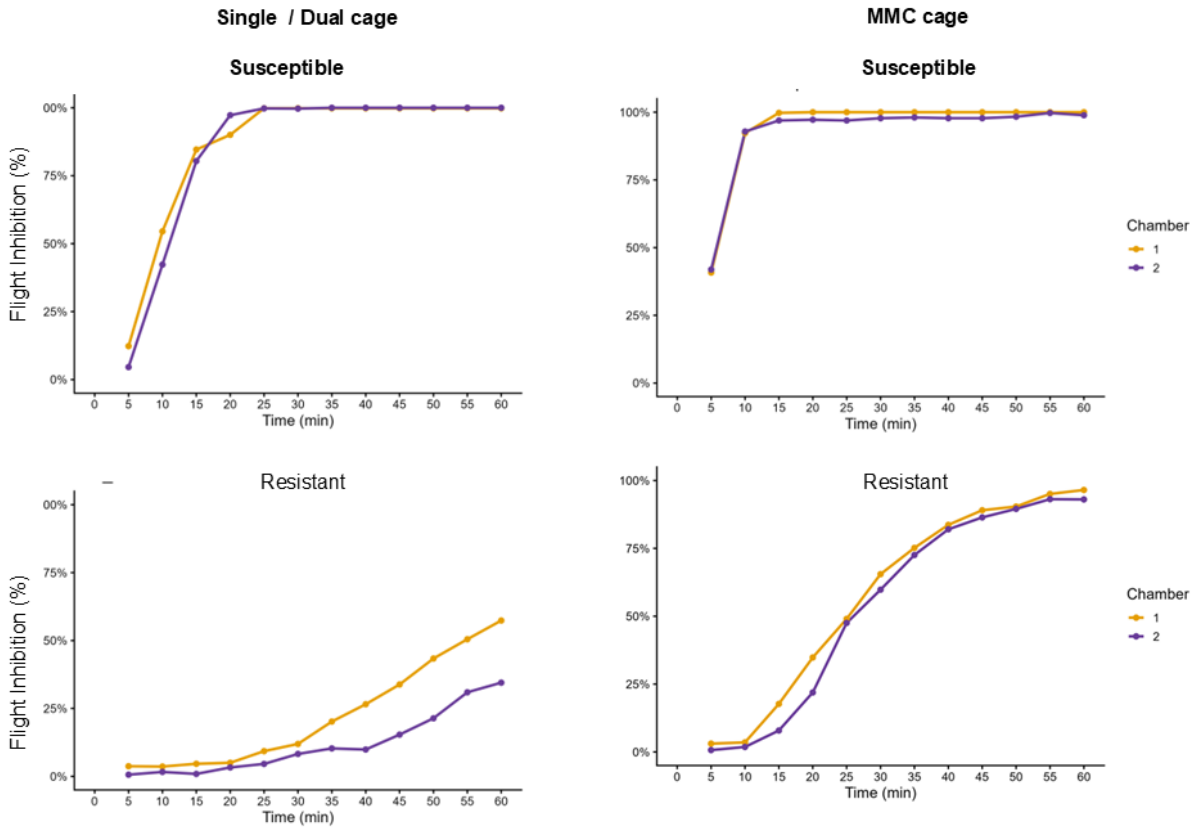

Figure S1. Time-response comparison between independent PG chambers. Cumulative flight inhibition (FI, %) over time in Chamber 1 and Chamber 2 across the experimental conditions evaluated. Panels show responses for susceptible and resistant mosquitoes under the different assay configurations.

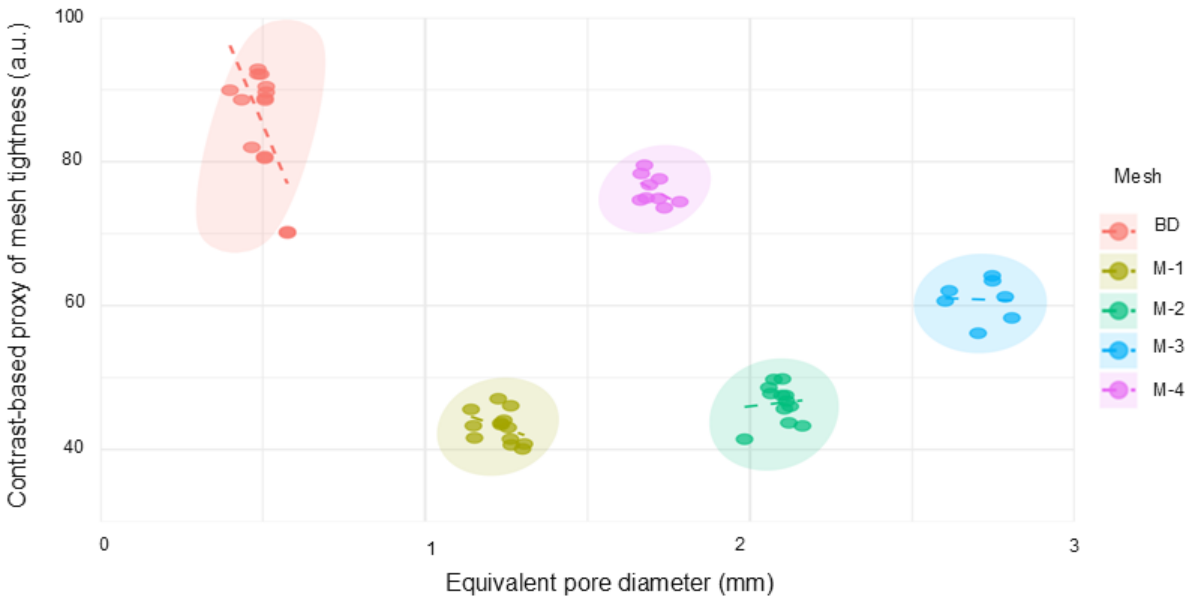

Figure S2. Physical characteristics of cage mesh materials used in the bioassays.
Relationship between equivalent pore diameter (mm) and contrast-based proxy of mesh tightness (arbitrary units, a.u.) for the five mesh types evaluated: BugDorm (BD) and MMC meshes (M-1 to M-4). Points represent individual pore measurements, dashed lines indicate fitted linear trends within each mesh type, and shaded ellipses represent the distribution of observations.

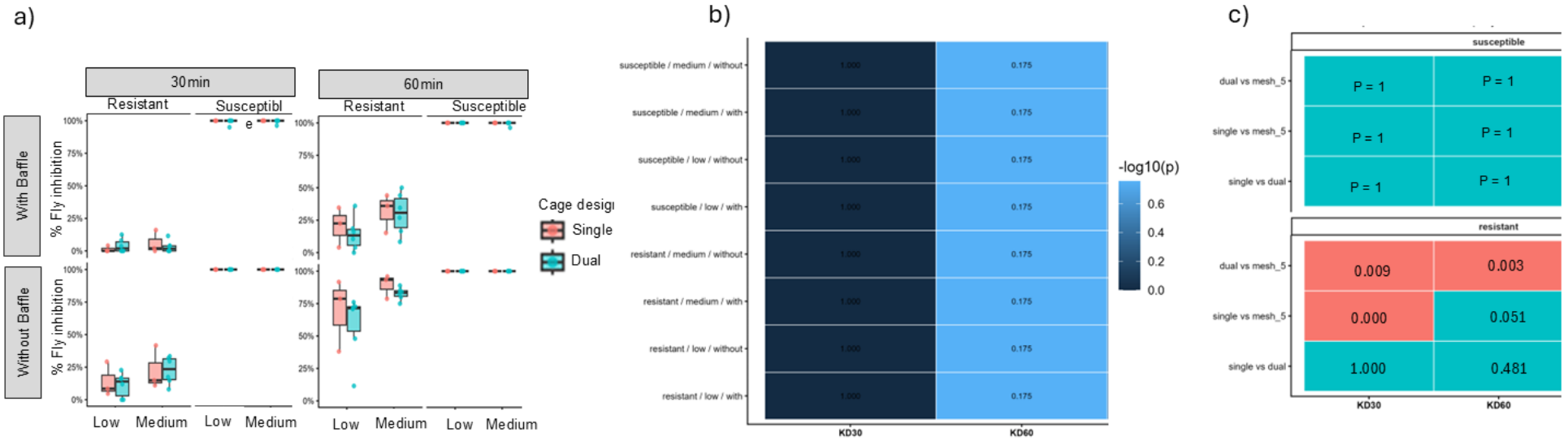

Figure S3. Influence of cage configuration on flight inhibition and reproducibility of bioassay responses. **(a)** Flight inhibition (FI, %) at 30 and 60 min in single- and dual-cage configurations under low and medium airflow conditions, with and without baffle ventilation. Boxplots show the median and interquartile range, and points represent individual replicates. **(b)**Significance levels associated with FI responses across mosquito strains, airflow intensities, and ventilation configurations (with and without baffle) at 30 min and 60 min. Values indicate adjusted P-values from statistical comparisons. **(c)** Pairwise comparisons of FI responses between single-, dual-, and MMC-cage configurations for susceptible and resistant mosquitoes at 30 min and 60 min. Values indicate adjusted P-values from post hoc comparisons.

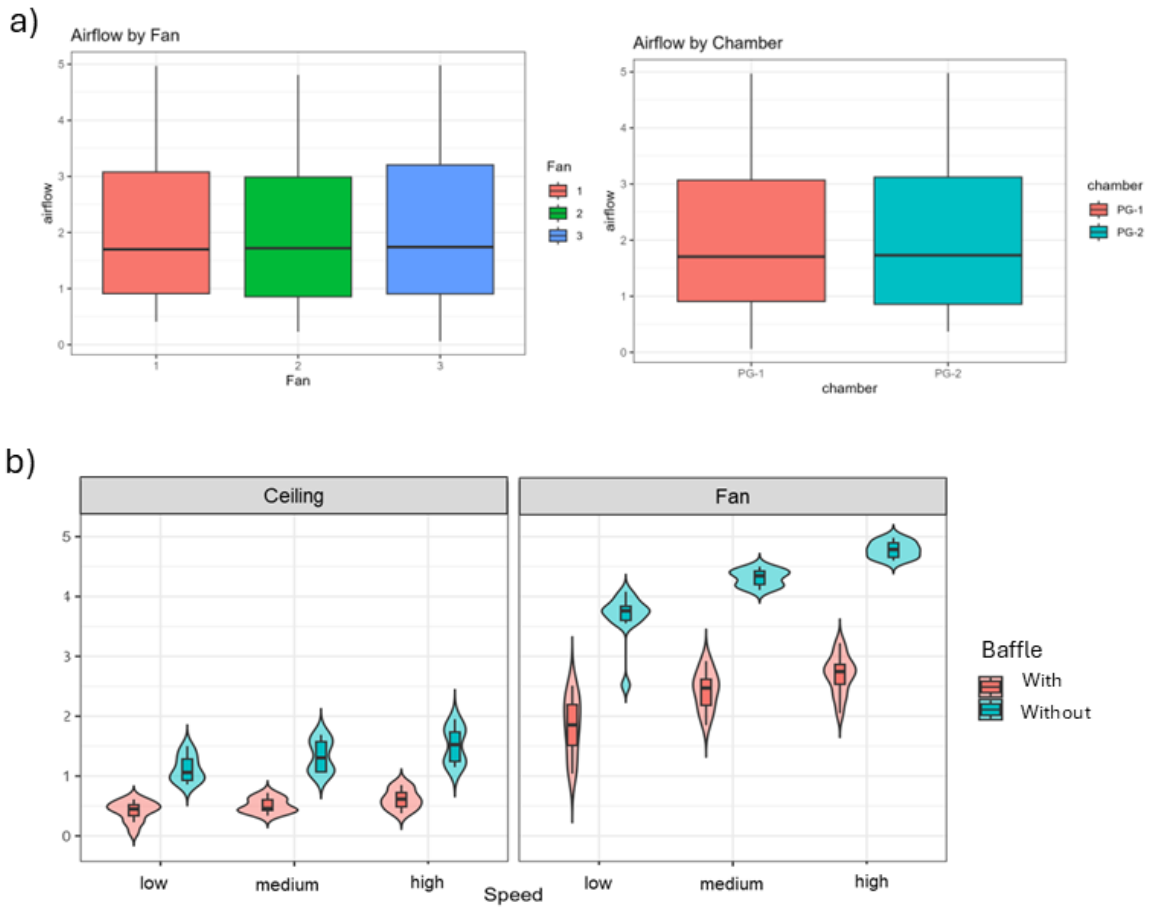

Figure S4. Characterisation of fan performance and chamber airflow. **(a)** Wind speed measurements recorded for the three fan units used in the study and across the two independent PG chambers. Boxplots show the median, interquartile range, and overall distribution of measurements. **(b)** Airflow velocity measurements recorded at ceiling and fan positions under low, medium, and high fan-speed settings, comparing conditions with and without cage mesh. Violin plots show the distribution of measurements, with embedded boxplots indicating the median and interquartile range.

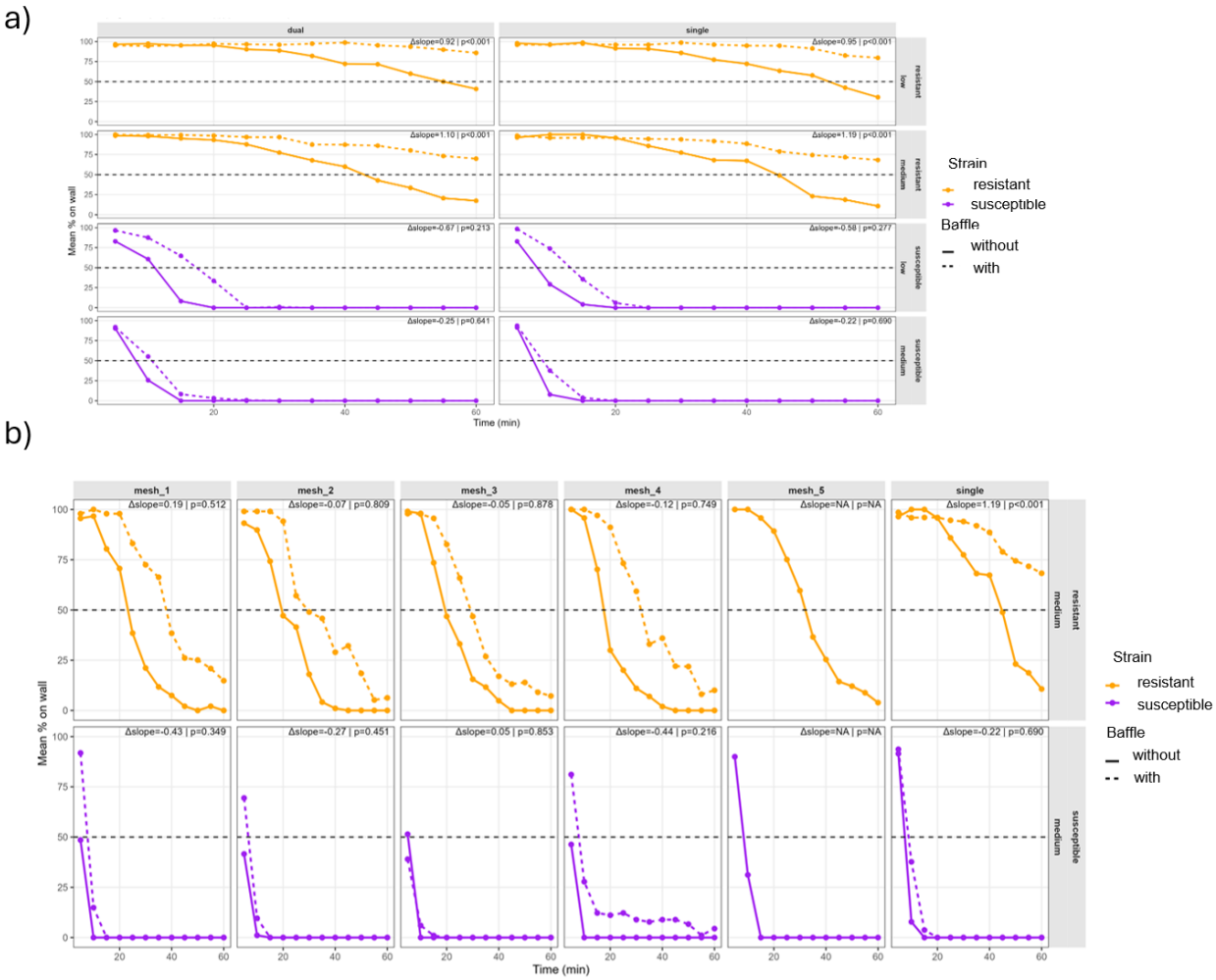

Figure S5. Time-response of flight inhibition under different ventilation and mesh configurations.
(a) Mean flight inhibition (FI, %) over time in single- and dual-cage configurations under low and medium airflow conditions, with and without baffle ventilation. (b) Mean flight inhibition (FI, %) over time across MMC mesh types and the standard single-cage configuration under medium airflow conditions. Separate panels show susceptible and resistant mosquitoes. Solid and dashed lines indicate ventilation conditions without and with baffle, respectively. Δslope values represent differences in FI trajectories between ventilation configurations.

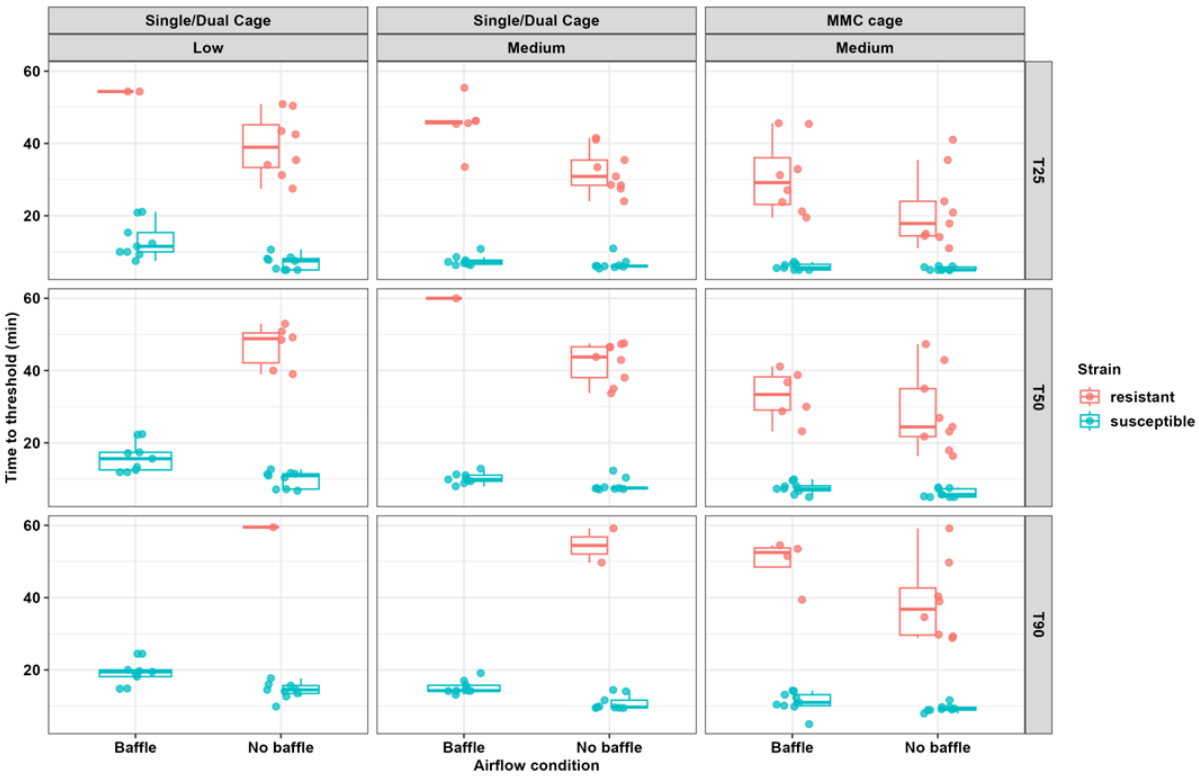

Figure S6. Time to flight inhibition thresholds across airflow and cage configurations.
Time required to reach 25%, 50%, and 90% flight inhibition (T25, T50, and T90) for susceptible and resistant mosquitoes exposed to transfluthrin passive emanators. Columns represent airflow and cage configurations (single/dual cage at low and medium airflow, and MMC cage at medium airflow), while rows indicate the FI threshold analysed. Airflow conditions were evaluated with and without baffle ventilation. Boxplots show the median and interquartile range, and points represent individual replicates.